

# Radiative Transfer in a Gas-Turbine Combustor

M.P. Mengüç,\* W.G. Cummings III,† and R. Viskanta‡  
*Purdue University, West Lafayette, Indiana*

A methodology is presented to predict radiative transfer in an axisymmetric cylindrical enclosure representing a typical gas-turbine combustor that contains radiatively participating gases and particles. Inhomogeneities of the radiative properties and temperature distribution of the medium are allowed for, and the boundaries are assumed to be diffusely emitting and reflecting. The effects of axial and radial variations of temperature and soot properties on radiative heat flux distributions at the wall are investigated. Film cooling is shown to have a marked effect on wall heat flux, especially when it quenches the soot oxidation process. Radiative flux at the wall is greater if the temperature of the medium is uniform, rather than if it has a center-peaked radial temperature profile.

## Nomenclature

$C_s$	= soot concentration, g/m <sup>3</sup>
$D$	= diameter of droplets, $\mu\text{m}$
FA	= fuel-air ratio
$f_v$	= soot volume fraction
$I$	= radiative intensity, W/m <sup>2</sup> -sr
$I_b$	= Planck's blackbody function, W/m <sup>2</sup> -sr
$I_i$	= moments defined by Eq. (6)
$m$	= mass, kg
$n$	= index of refraction
$Q$	= efficiency factor
$\vec{q}$	= radiative heat flux vector, kW/m <sup>2</sup>
$P$	= pressure, atm
$R$	= gas constant
$r$	= radial coordinate
$r_0$	= radius of a cylindrical enclosure, see Fig. 1
$T$	= absolute temperature, K
$z$	= axial coordinate
$z_0$	= length of a cylindrical enclosure, see Fig. 1
$\beta$	= extinction coefficient, m <sup>-1</sup>
$\delta$	= Kronecker delta function
$\epsilon$	= wall emissivity
$\eta$	= direction cosine in the $\phi$ direction, Eq. (2)
$\theta$	= polar angle
$\kappa$	= absorption coefficient, m <sup>-1</sup>
$\lambda$	= wavelength of radiation
$\mu$	= direction cosine in the $z$ direction, Eq. (2)
$\xi$	= direction cosine in the $r$ direction, Eq. (2)
$\rho$	= soot density, kg/m <sup>3</sup>
$\sigma$	= Stefan-Boltzmann constant; also scattering coefficient, m <sup>-1</sup>
$\phi$	= azimuthal angle; also, equivalence ratio
$\Phi$	= scattering phase function
$\chi$	= dimensionless radius, $r/r_0$
$\Psi$	= function defined by Eq. (4)
$\omega$	= single-scattering albedo, $1 - (\kappa/\beta)$
$\Omega$	= solid angle, see Fig. 1

## Subscripts

$a$	= air
conv	= convective
$f$	= fuel
$g$	= gas
$m$	= mean values
$P$	= Planck's mean
rad	= radiative
$s$	= soot
$w$	= wall

## Introduction

A MAJOR operating cost of aircraft turbine engines is the replacement of combustor liners after relatively short periods of use. Damage is usually in the form of cracks, which develop at discontinuities in the wall such as cooling slots and air admission holes or at locations where manufacturing processes produce severe residual stresses.

Damage from high metal temperatures could be better avoided if a reliable method of estimating liner wall temperature were known. For the purpose of analysis, a liner may be regarded as a container filled with hot flowing combustion gases surrounded by a casing. Between the container and the casing flows relatively cool air. The liner is heated by radiation and convection from the hot gas-soot mixture inside and is cooled by radiation to the outer casing and by convection to the annulus air. The relative proportions of the radiation and convection components depend upon the geometry and operating conditions of the engine; however, typically, radiation accounts for 30-50% of the overall heat flux to the walls in present-day engines. As fuels of an increasingly soot-forming nature are used, the radiative contribution may reach up to 80% of the total wall heat flux.

Of the four heat-transfer processes that govern liner wall temperature, three (internal convection, external convection, and external radiation) can be calculated with reasonable confidence. However, it is quite difficult to model the internal radiation with the same level of accuracy. The multidimensionality of the radiative field must be taken into account to accurately predict the heat transfer to the liner walls by radiation from the flame.

With the calculation schemes used today, only rough estimates of liner wall temperature, and, hence, liner durability, can be made. This is because the currently available methods, which are based on a mean-beam-length approach, can predict only average radiation heat flux at the liner surface.<sup>1</sup> The simple methods are incapable of predicting the local radiation flux within the combustor; furthermore, they cannot account for radial and axial nonuniform-

Received May 21, 1985; presented as Paper 85-1072 at the AIAA 20th Thermophysics Conference, Williamsburg, VA, June 19-21, 1985; revision received Dec. 18, 1985. Copyright © American Institute of Aeronautics and Astronautics, Inc., 1985. All rights reserved.

\*Graduate Research Assistant, School of Mechanical Engineering; presently, Assistant Professor of Mechanical Engineering, Department of Mechanical Engineering, University of Kentucky, Lexington, KY.

†Graduate Student, School of Mechanical Engineering. Member AIAA.

‡Professor of Mechanical Engineering, School of Mechanical Engineering. Associate Fellow AIAA.

mities of the temperature and the radiative properties of the soot-gas mixtures. This is a serious shortcoming because the combustor designer allocates film cooling air based on these calculations. In the absence of accurate heat flux predictions one must overprotect the liner. Too much cool air near the walls, however, can reduce combustion efficiency, increase pollutant emissions, and distort the temperature pattern at the combustor outlet, which stresses the turbine blades. An extensive review<sup>2</sup> of multidimensional radiative transfer models has been given recently; therefore, it will not be repeated here.

In this paper the radiation heat flux distributions to the liner walls from the soot and combustion gases in the combustor are calculated using the radiation heat-transfer model developed recently.<sup>3</sup> This model is for finite, axisymmetric, cylindrical enclosures and employs the first- or third-order spherical harmonics approximations (i.e.,  $P_1$  or  $P_3$  approximations, respectively). The governing equations of the model are elliptic partial differential equations solved using an accurate finite difference scheme. The model accounts for the inhomogeneities in the temperature of the medium, the wall temperature, and the radiative properties of the medium, such as extinction coefficient, single scattering albedo, etc. Earlier validation studies have shown that if the smallest optical dimension of the medium is greater than 0.5, the accuracy of the method is better than 90%. Therefore, this radiative heat-transfer model is quite appropriate for obtaining improved understanding of radiative heat transfer in a gas-turbine combustor. By performing sensitivity analyses on a typical gas-turbine combustor model, the authors have determined which operating parameters have the greatest effect on radiative transfer within the combustor and on radiation flux to the liner walls.

In the literature there are several experimental works on gas-turbine combustors. Najjar and Goodger<sup>4</sup> found that flame radiation to the liner increased negligibly for soot concentrations above 25 g/m<sup>3</sup>. Kuznar et al.<sup>5</sup> concluded that fuels of higher carbon-to-hydrogen ratio gave a higher heat flux to the wall and a higher wall temperature. They measured a lower gas temperature, however, near the wall when burning the low-hydrogen fuel. Claus et al.<sup>6</sup> determined that the effect of lower hydrogen fuels was an increase in soot, but this increase was less noticeable at higher pressures and at large axial distances from the injector. Experimental results have at times been contradictory. A frequent cause of this has been the interdependence of various parameters on one another. To isolate the effects of temperature and soot concentration on the radiative heat flux at the liner, then, has been a major goal of this work. As will be seen, some of the chosen profiles for soot and especially temperature would be unlikely to occur in an actual combustor. We have used them, nonetheless, because they clearly illustrate the sensitivity of flame radiation to isolated model parameters and provide improved understanding of radiation transfer in a combustor.

## Analysis

### Formulation

The gas-turbine combustor is modeled as an axisymmetric cylindrical enclosure containing radiatively participating

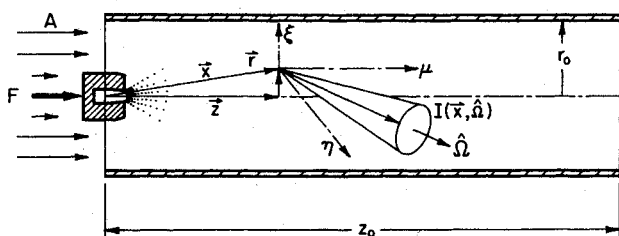


Fig. 1 Typical gas-turbine combustor:  $r_0 = 6.69$  cm,  $z_0 = 45.7$  cm.

gases and soot particles. Cylindrical enclosures have one advantage in that, for practical purposes, they may be considered to be axisymmetric. As a result, the radiative transfer equation (RTE) is to be solved in two dimensions rather than three.

For an absorbing, emitting, and anisotropically scattering gas-particle mixture in local thermodynamic equilibrium, the time-independent spectral RTE for two-dimensional, axisymmetric cylindrical enclosures is given by<sup>7</sup>

$$\left[ \frac{1}{\beta} \left( \xi \frac{\partial}{\partial r} - \eta \frac{1}{r} \frac{\partial}{\partial \phi} + \mu \frac{\partial}{\partial z} \right) + 1 \right] I(r, z, \theta, \phi) = (1 - \omega) I_b [T(r, z)] + \frac{\omega}{4\pi} \int_0^{2\pi} \int_0^\pi I(r, z, \theta, \phi) \Phi(\theta, \phi; \theta', \phi') \sin \theta' d\theta' d\phi' \quad (1)$$

The subscript  $\lambda$  denoting spectral quantities in the RTE has been left off for the sake of clarity, but it is implied. In this equation  $\phi$  corresponds to the difference of the azimuthal angles, such as  $\phi = \phi_\Omega - \phi_r$ . The direction cosines are given by

$$\xi = \cos \phi \sin \theta, \quad \eta = \sin \phi \sin \theta, \quad \mu = \cos \theta \quad (2)$$

At this point we can introduce the spherical harmonics approximation for the radiative intensity and write the RTE in terms of moments of intensity. Details of the analysis are given in two previous publications,<sup>3,8</sup> therefore, they will not be repeated here. The introduction of the spherical harmonics approximation reduces the integrodifferential equation, Eq. (1), to a series of elliptic partial differential equations. The  $P_3$  approximation solves as many as four partial differential equations. The solution of these equations has been obtained numerically by an accurate finite difference scheme using a general computer code ELLPACK.<sup>9</sup> The ELLPACK code was developed at Purdue University and is a proprietary, general elliptic, partial differential equation solver. The accuracy of the finite difference scheme used is  $O(\Delta r^2 + \Delta z^2)$ .

### Physical Model

In order for this analysis to be comparable to experimental data from an actual gas turbine, operating conditions from such an engine were applied to the computational model. Mean temperature and soot profiles were taken from the work of Najjar and Goodger.<sup>4</sup> In their experiments they measured flame radiation from several different fuels, three of which were selected for this study: kerosene, a modern jet fuel; R25, a blend of 75% gas oil and 25% residual fuel oil; and R50, a 50/50 mixture of gas oil and residual fuel oil. Their combustor was of the same dimensions as the cylinder used in the present analysis (see Fig. 1). The different fuels yielded different soot and temperature distributions, see Fig. 2. These profiles were obtained by curve-fitting to the experimental data reported by Najjar.<sup>10</sup>

It is generally accepted that at pressures found within a gas-turbine combustor, emission from water vapor and carbon dioxide is much less than the continuous emission from the soot particles. In this paper, then, only soot emission is considered. The soot absorption coefficient can be obtained from Mie theory<sup>11</sup> in the small particle limit using the complex index of refraction data. However, for many different soot samples, the following approximate relation holds<sup>12</sup>:

$$\kappa_\lambda = 7(f_v/\lambda) \quad (3)$$

Starting from this expression, Planck's absorption coefficient for soot has been calculated at several temperatures, and a curve-fitted polynomial  $\Psi(T)$  has been obtained that

is given as

$$\Psi(T) = \sum_{i=0}^3 d_i T^i \quad (4)$$

where

$$\begin{aligned} d_0 &= -0.253475 \times 10^4 & d_1 &= 0.272464 \times 10^3 \\ d_2 &= -0.928538 \times 10^{-2} & d_3 &= 0.123273 \times 10^{-5} \end{aligned}$$

This expression is in very good agreement with the calculated values (within 2% in the temperature range of 400-2400 K). Then, the temperature-dependent mean absorption coefficient is given as

$$\kappa_{p,s} = 7f_v \Psi(T) = 7(C_s/\rho) \Psi(T) \quad (5)$$

where  $\rho$  is the density of soot particles, taken as  $1.65 \text{ g/cm}^3$ . Note that this value is based on experiments, and its use is more reasonable than a value of  $\rho = 2.0 \text{ g/cm}^3$ , which is closer to the density of pure graphite.<sup>10</sup>

The radial distributions of temperature and soot concentration were not available from the experimental work.<sup>4,10</sup> In order to examine the effect of radial variation of temperature or soot concentration on the radiative flux distribution, the following function was employed:

$$\Gamma(\chi) = C(1 - \chi^{1/k}) \Gamma_{\text{avg}} \quad (6)$$

where  $\Gamma$  corresponds to either temperature  $T$  or soot concentration  $C_s$ , the subscript "avg" stands for the radially averaged values, and  $C$  is the coefficient, such that

$$C = \left[ \sum_{i=0}^n \frac{(-1)^i}{[i/k + 1]} \frac{n!}{(n-i)! i!} \right]^{-1/n} \quad (7)$$

This coefficient is obtained from the definition of mean value as

$$\Gamma_{\text{avg}} = \left[ \int_0^1 \Gamma^n(\chi) d\chi \right]^{1/n} \quad (8)$$

The value of  $k$  is the order of the polynomial curve. In this study  $k$  values of 0 and  $1/3$  were chosen for temperature, while 0,  $1/3$ , and 2.0 were selected for soot. For the soot concentration profile the exponent  $n$  is taken as 1, whereas for the temperature distribution  $n$  is taken as 4. In Fig. 3, one radial profile for the temperature distribution and two profiles for the soot concentration are shown graphically.

It is recognized that the Planck mean may not be the most appropriate absorption coefficient for predicting radiative transfer in the combustor on the gray basis; however, if the gray medium approximation is not made, the calculations will have to be performed on a spectral basis. In view of the fact that the temperature and radiating species concentration distributions are not known precisely, use of the approximation appears to be justified.

### Results and Discussion

In this study several parameters are investigated. The first is soot concentration, which accounts for variation in the sooting tendency of the burning fuel. Values range from one typical of a nonluminous flame to one for a very yellow flame, which has a high soot concentration. The second parameter is the combustion product temperature, which affects the radiative flux in two ways: 1) the absorption coefficient of the soot formed and 2) the emitted blackbody flux of the medium. In practice this is brought about by a change in the fuel-to-air ratio or a change in combustor inlet conditions. The third parameter studied is the radial temperature profile. A single fuel injector produces a hot, centrally

located core of flame gases surrounded by relatively cool gases; multipoint atomizers, on the other hand, give more nearly uniform temperature distributions. Finally, the effect of the liquid fuel droplets on scattering of radiation has been examined. Other parameters have been investigated too, namely, wall emissivity and liner temperature distribution. For a wide range of reasonable values of these parameters, however, their effects on radiative heat transfer were not significant; therefore, for the sake of brevity they are not

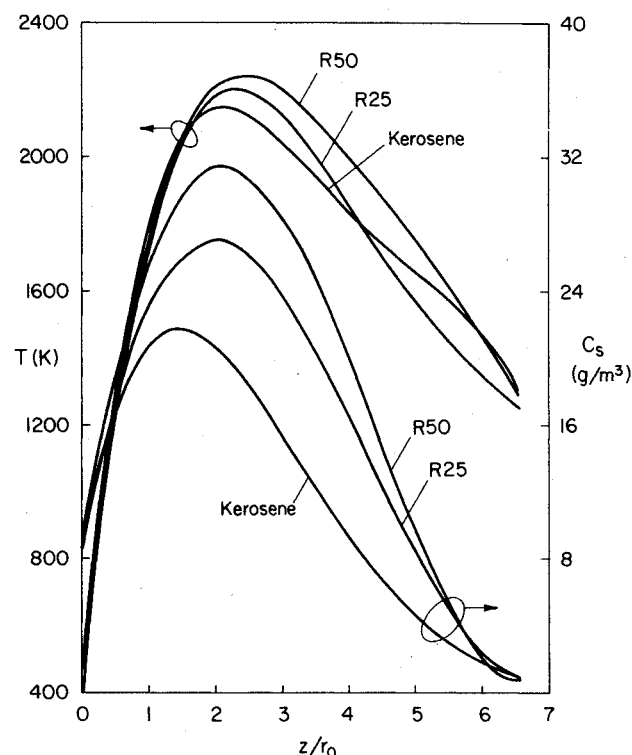


Fig. 2 Axial temperature and soot concentration distributions for kerosene, R25, and R50 fuels.

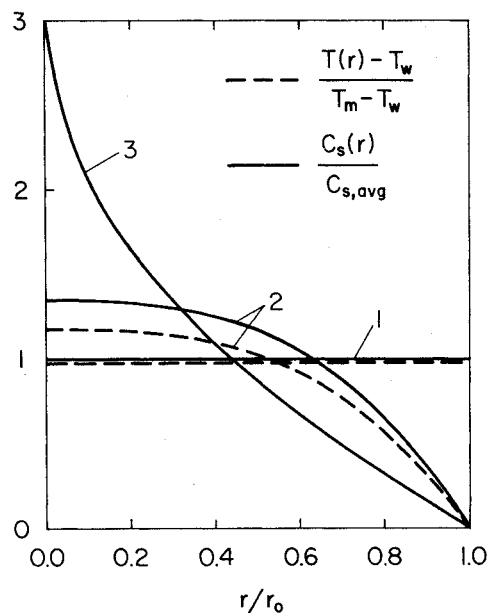


Fig. 3 Normalized radial profiles for temperature and soot concentration. For temperature,  $n=4$ ; for soot concentration,  $n=1$ : 1- $k=0$  (radially uniform), 2- $k=1/3$ , and 3- $k=2.0$ .

discussed in this paper. Their values were fixed at the following:  $T_w = 923$  K and  $\epsilon = 0.8$ .

It is recognized that not only the average temperature and radiating species (soot,  $\text{CO}_2$ ,  $\text{H}_2\text{O}$ , and fuel droplets) but also their axial and radial distributions as well as the radiation properties of the combustor walls affect radiative transfer in the combustor. Unfortunately, detailed distributions of these parameters do not appear to have been determined; therefore, plausible distributions of the important model parameters (i.e., temperature and soot) have been postulated for this investigation. Parametric calculations were then performed to determine the sensitivity of radiative transfer in a combustor to these important model parameters.

#### Effects of Radial Temperature Distribution

In Fig. 4, the radiative fluxes to the cylindrical walls calculated for uniform and radially varying (profile 2 of Fig. 3) medium temperatures are compared. The temperature profile impacted wall heat flux in several significant ways. A medium of uniform temperature produced more than twice as large a radiative flux at the liner walls at peak, as did the tapered profile of the same average energy content. Note that here the soot concentration was assumed to be uniform for both temperature distributions; however, the absorption coefficient of the medium varied with the temperature for the tapered profile, while remaining constant for uniform temperature. A direct result of this was the unexpectedly higher radiative flux from kerosene than from the R25 and R50 blends, at peak, when the temperature profile was nonuniform. In practice such a nearly uniform soot concentration profile, though unlikely, might come about if the film cooling air of the combustor penetrated into the combustion zone sufficiently to quench the soot oxidation process. A cloud of soot would then blanket the liner wall; furthermore, for the fuel of higher  $C/H$  ratio, this cloud would be more strongly absorbing. It would, therefore, actually

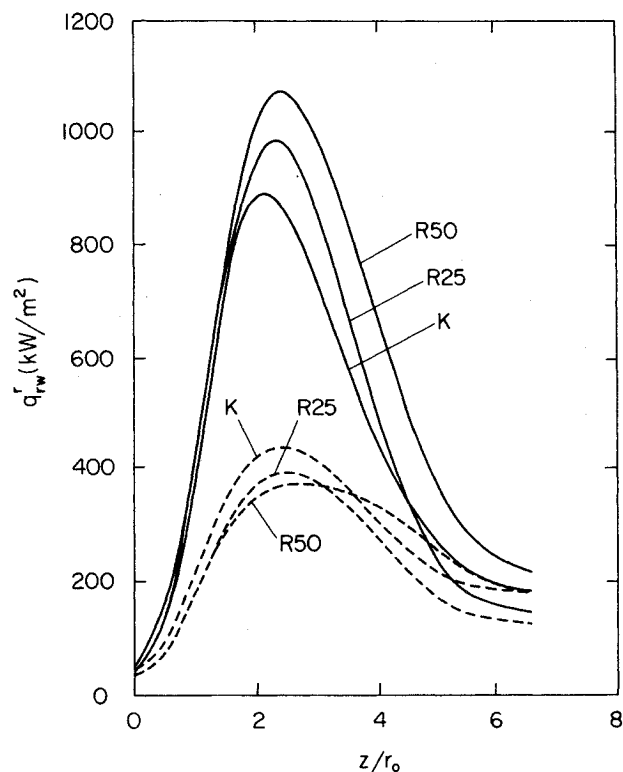


Fig. 4 Effect of fuel type and radial variation of temperature on the radiative heat flux distribution on the cylindrical wall (K refers to kerosene): solid line, radially uniform temperature; dashed line, radially variable temperature.

keep the wall cooler than kerosene's soot. Only if this blanket remained quite hot as it flowed downstream would it overtake kerosene's hot core of soot as an emitter. This is just what R50 has been shown to do (Fig. 4).

The effect of radial temperature profile on the radiative heat flux distribution at four axial locations is shown in Fig. 5 for kerosene and R50 fuels. For the uniform temperature profile, the radiative heat flux became larger toward the wall because of the strong emission of radiation by the combustion products in the vicinity of the cylindrical walls. Of course, a high soot concentration is undesirable in the engine exhaust; the point here, though, is that the designer should observe that a reduction in the film-cooling airflow greatly intensifies the heat flux to the liner wall, the intensification being more pronounced for sootier fuels (see Fig. 5). This demonstrates the importance of the properties of the combustion products in the region near the wall.

The time-averaged energy equation for the combustion gases can be expressed in the following general form:

$$\text{div}(\rho \vec{v} \bar{\phi}) = \text{div}(\Gamma_{\phi} \text{grad} \bar{\phi}) - \text{div} \vec{q}^r \quad (9)$$

where the time-averaged variable  $\bar{\phi}$  could stand for stagnation enthalpy,  $\vec{v}$  the velocity vector,  $\Gamma_{\phi}$  the effective diffusion coefficient accounting for turbulence, and  $\vec{q}^r$  the radiation flux vector. It is clear that determination of the temperature distribution in a combustor requires knowledge of the radiative flux divergence,  $\text{div} \vec{q}^r$ . In order to obtain a feel for the magnitude of the radiative contribution to the overall thermal energy balance some results are given in Fig. 6. The results show that the divergences are quite large, negative in some and positive in other regions of the combustor. This suggests that the interaction between convection and radiation could not be neglected when calculating the

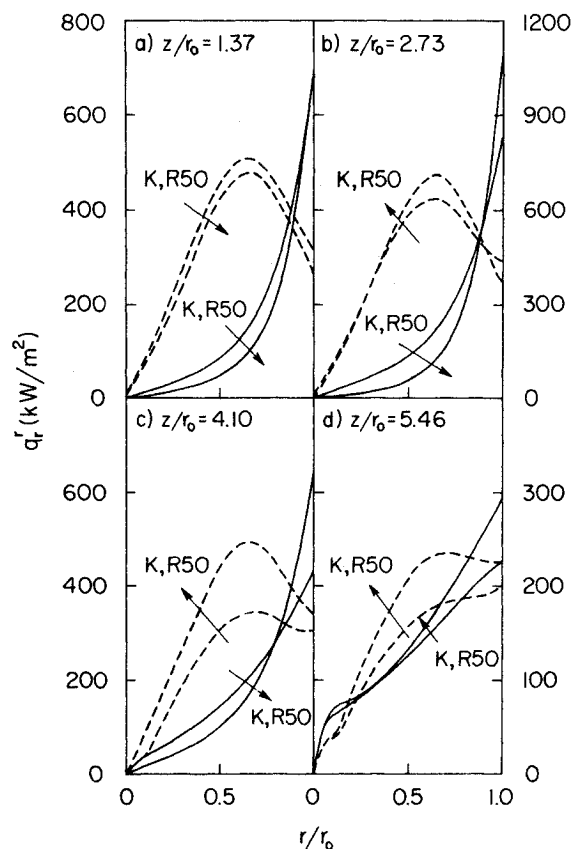


Fig. 5 Effect of type and radial variation of temperature on the radiative heat flux distributions at four axial locations (K refers to kerosene): solid line, radially uniform temperature; dashed line, radially variable temperature.

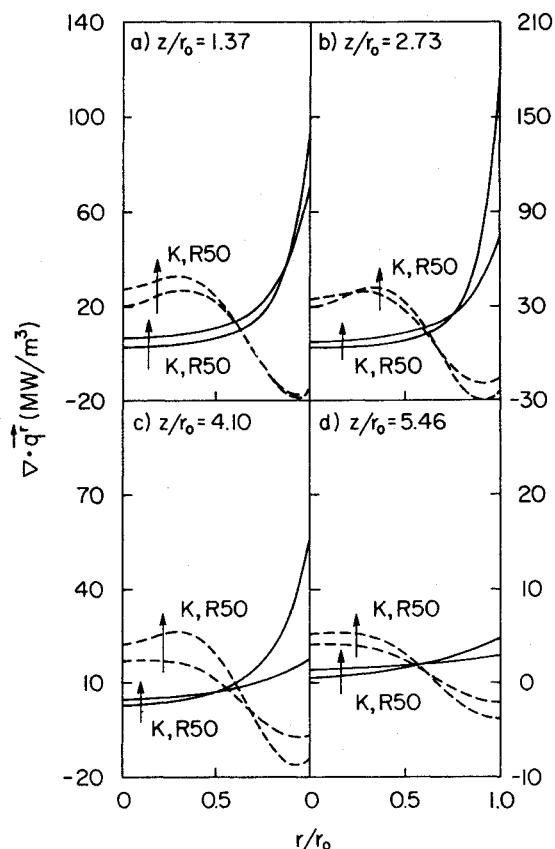


Fig. 6 Effect of fuel type and radial variation of temperature on the divergence of radiative heat flux distributions at four axial locations (K refers to kerosene): solid line, radially uniform temperature; dashed line, radially variable temperature.

temperature (enthalpy) distribution in the combustor. The results of Fig. 6 further demonstrate the importance of the radial and axial temperature distributions on the radiative flux divergences. The divergences are strongly dependent on the soot concentration and temperature distributions in the combustor, particularly in the region near the wall. Indeed, this is where film cooling effects are most pronounced in an operating combustor.

#### Effects of Radial Soot Concentration Distribution

In Figs. 7 and 8, the effect of radial soot concentration distribution on the radiative heat flux distributions to the cylindrical wall as well as in the medium is shown. Just as the total energy along a diameter was held constant for the different temperature profiles, so the total soot volume fraction was maintained for three different radial profiles of soot concentration (see Fig. 3). In all three cases given in Fig. 7, the temperature was assumed to be uniform. Because the total soot concentration was always the same, an increase in the centerline concentration necessarily created a decrease in the value near the wall. The consequence of the tapered profile, then, was to increase the radiative heat flux at the wall. The reason for this was that the soot cloud near the cylindrical walls exhibited less self-absorption. In effect, the wall received irradiation from deeper within the cylindrical combustion chamber, and the radiative flux increased as the liner wall was approached. For values of  $k$  ranging from  $1/3$  to  $2.0$  the effect on the order of the polynomial soot curve was less than the effect of the change in total soot volume fraction with a change in fuel type (see Fig. 2).

Figure 8, which depicts the radial radiative flux distributions at four axial locations in the medium for kerosene and R50 fuels, shows that for the radially varying soot profile the heat flux increased dramatically toward the wall. The reason for this was that the thinner soot cloud near the cylindrical

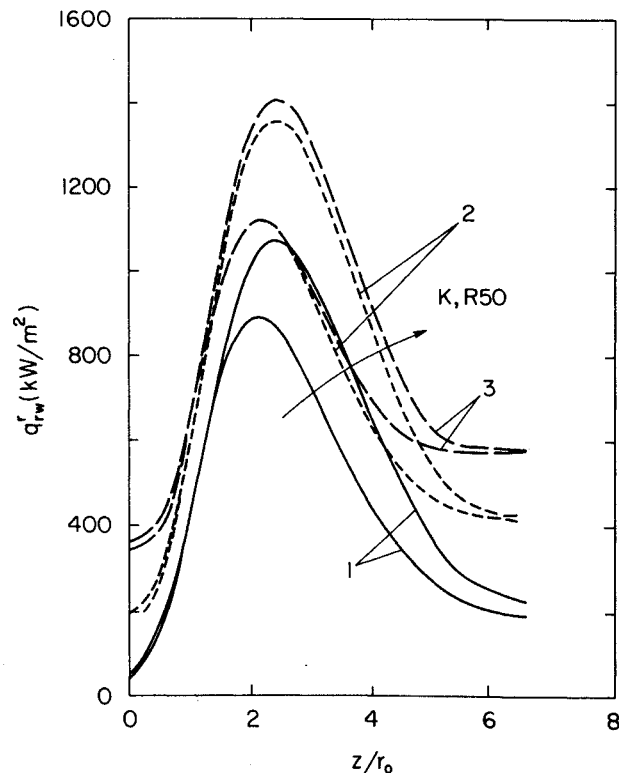


Fig. 7 Effect of fuel type and radial variation of soot concentration distribution on radiative heat flux distribution on the cylindrical wall (K refers to kerosene): 1- $k=0$  (radially uniform), 2- $k=1/3$ , and 3- $k=2.0$ .

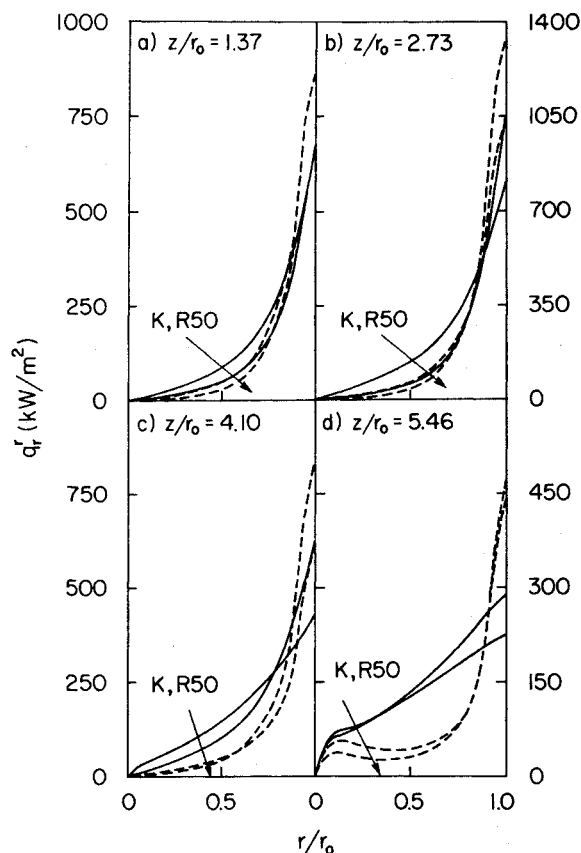


Fig. 8 Effect of fuel type and radial variation of soot concentration distribution on radial radiative heat flux distribution at four axial locations (K refers to kerosene): solid line, radially uniform ( $k=0$ ); and dashed line, radially nonuniform ( $k=2.0$ ).

wall absorbed much less of the wall-bound emission than that of the uniform distribution.

#### Effect of Scattering by Fuel Droplets

The effect of scattering of radiation by liquid fuel droplets just downstream of the atomizer has been examined. The evaporation distance for the central, conical spray was 6 cm, and the Sauter mean diameter of the droplets was assumed to be 25  $\mu\text{m}$ . The single-scattering albedo was obtained as a function of equivalence ratio, and it was noticed that it may have a value between 0.5 and 0.9. The analysis related to scattering coefficients is summarized in the Appendix. Even with liberal estimates for all of the parameters considered, the effect of scattering by spray had a very small effect on the radiative flux distributions. This is mainly because of the small volume of the spray, which occupies only a fraction of the combustor volume. From this we can conclude that, for all practical purposes, the effect of scattering by droplets on radiation heat transfer in gas-turbine combustors can be neglected.

#### Comparisons with Other Data

The results of Claus et al.,<sup>6</sup> if interpolated slightly to match the present inlet conditions, agree to within 10% of the predictions for the nonuniform temperature profile and kerosene fuel for  $k = 1/3$ . In contrast to the predictions, however, they found that the sootier fuel resulted in a higher radiative flux to the wall than did the cleaner fuel. This probably indicates a minimal penetration of film cooling air such that the soot concentration was not uniform across the diameter of the combustor.

The predictions, when compared to the data of Najjar and Goodger,<sup>4</sup> are in poorer agreement for the tapered temperature profile. These authors, however, admitted that cold pockets along the diameter of observation lowered their radiative flux measurements. On the other hand, the radial temperature profile used here is somewhat arbitrary. Therefore, some discrepancy was expected. Again, the measured flux increased with increasing  $C/H$  ratio, pointing out that a uniform radial soot concentration profile, although useful heuristically, did not arise in the actual combustor.

Manufacturers of gas-turbine engines typically treat the wall heat flux as the sum of the radiative and convective fluxes. The radiation can be estimated with a mean-beam-length method,<sup>13</sup> while the convection is calculated via a modified Nusselt analysis.<sup>14</sup> The base data for the mean heat-transfer calculations and the results for the three different fuels, burning at  $P = 10$  atm and at a uniform, peak temperature, are given in Tables 1 and 2.

In Table 2, the average radiative heat flux calculated from the  $P_3$  model is given as a range for each fuel rather than a single value. The lower limit of each range corresponds to a uniform distribution (profile 1) of soot, and the upper limit corresponds to the radial profile 3, as shown in Fig. 3. Note that the radiative fluxes calculated from the mean-beam-length (global) method for kerosene are in agreement with the  $P_3$ -model results. However, this may be fortuitous; the mean-beam-length method is not expected to yield accurate radiative transfer predictions if there are significant radial temperatures and soot concentration variations in the combustor. Also, the simple approach is not able to predict the local radiative flux to the liner wall. Another important difference between the radiative heat fluxes calculated from the model and the mean-beam-length method is that the former is resolved into positional and directional values. These vary by up to 100% from the average values, and the portion of a combustor liner that has the greatest heat flux must be designed to withstand that intense heating. A one-dimensional ("plug flow") analysis could be employed. Such an analysis may predict maximum radiative heat fluxes but is

**Table 1** Base data for mean heat-transfer calculations  
( $P = 10$  atm,  $T_w = 923$  K,  $\phi = 1.0$ ,  $\epsilon_w = 0.8$ ,  $\dot{m}_{pz} = 0.4$  kg/s)

Fuel	$C/H$	$\epsilon_g$	$T_g$ , K
Kerosene	6.48	0.602	2150
R25	6.95	0.677	2210
R50	7.13	0.695	2250

**Table 2** Radiative and convective heat fluxes, kW/m<sup>2</sup>

Fuel	Mean calculations		$P_3$ model
	$q''_{\text{conv}}$	$q''_{\text{rad}}$	$q''_{\text{rad}}$
Kerosene	606	577	441-717
R25	658	731	441-681
R50	700	811	526-795

likely to be poor in regions where the flame temperature is low and radiative transfer from hotter regions is important.

#### Conclusions

Based on the analysis presented and the results obtained, the following conclusions can be drawn:

1) A radially uniform temperature distribution resulted in more than twice the radiant wall heat flux at the point of maximum intensity as did a center-peaked profile of the same total energy. This means that in order to calculate radiative heat flux in a gas-turbine combustor accurately, one has to know the radial distribution of the temperature in the medium. Indeed, the radial temperature distribution had greater impact on the total radiative heat flux than even the type of fuel for the conditions and fuels examined in this study.

2) For uniformly distributed soot but tapered temperature profile, a sootier fuel may produce a smaller radiant heat flux at the walls (compare, for example, the kerosene and R25 results in Fig. 4). In practice, this would arise only with poor film cooling, i.e., very high film penetration. For the preceding reason a slight reduction in film cooling flow could significantly aggravate the thermal stress on the liner wall, especially for a sooty fuel.

3) Uniformly distributed soot with uniform temperature yielded a radiant flux 25-30% smaller than a center-peaked soot distribution; however, soot profiles with values of  $k$  from  $1/3$  to 2.0 in the polynomial representation of the profile had little impact on the radiative flux.

4) The radiative heat flux at the liner wall is strongly affected by the radial temperature and soot concentration distributions. This suggests that accurate flux predictions will require realistic modeling of the radial distributions of these parameters.

5) The average radiative heat flux calculated from the  $P_3$  model compared reasonably well with results based on mean-beam-length calculations presently used in the gas-turbine industry. The  $P_3$ -model results, however, were able to pinpoint locations of maximum radiative heat flux on the liner wall.

6) Scattering of radiation by the fuel droplets in a gas-turbine combustor can be safely neglected for all practical purposes.

7) A designer could implement a sensitivity analysis similar to the one used in this paper to examine the effects of changed fuel/air ratio, temperature pattern factor, sooting tendency, inlet air properties, etc.

Note that all of the conclusions drawn are based on the limited amount of sensitivity analysis described in the paper. Before using these conclusions for any practical system, it is recommended that a similar methodology be applied to the particular system under consideration to obtain specific conclusions.

### Appendix: Relation Between the Fuel Equivalence Ratio and Scattering Parameters

If all of the fuel sprayed into the combustor does not vaporize instantaneously, then the scattering of radiation should be considered along with the emission and absorption. Since in the experiments using the Schmidt technique only the extinction of radiation is detected, it is difficult to separate absorption from scattering. However, in theoretical calculations accounting for only absorption of radiation and neglecting the scattering may yield erroneous results. In this Appendix an analysis is presented to relate the equivalence ratio to the single-scattering albedo by assuming that the total extinction anywhere in the medium does not change.

The extinction coefficients, and their relations to the single-scattering albedo  $\omega$ , are given as

$$\beta = \sigma + \kappa, \quad \omega = 1 - \kappa/\beta \quad (\text{A1})$$

where  $\kappa$  and  $\sigma$  are absorption and scattering coefficients, respectively. The scattering coefficient is related to the number density  $N_D$  such that

$$\sigma = \pi (D_m^2/4) Q_s N_D \quad (\text{A2})$$

where  $D_m$  is the mean droplet diameter and  $Q_s$  the scattering efficiency factor. For nonabsorbing spheres,  $Q_s$  can be expressed as<sup>11</sup>

$$Q_s = 2 - \frac{4}{u} \sin u + \frac{4}{u^2} [1 - \cos u] \quad (\text{A3})$$

with

$$u = 2x(n-1) = \frac{2\pi D_m}{\lambda} (n-1) \quad (\text{A4})$$

Here,  $x$  is the so-called size parameter,  $\lambda$  the wavelength of radiation, and  $n$  the index of refraction for the fuel droplets.

By taking  $\lambda = 3 \mu\text{m}$ ,  $n = 1.4$ , and  $D_m = 25 \mu\text{m}$ , it is found that

$$u = 20.94, \quad Q_s = 1.848$$

Then, the number density is obtained from Eq. (A2). The mass of fuel droplets is calculated from

$$m_f = \rho V N_D \pi D_m^3/6 \quad (\text{A5})$$

and the mass of air from

$$m_a = \rho V = PV/RT \quad (\text{A6})$$

By assuming that the spray is conical and scattering droplets exist only for the first 5 cm of axial distance, starting from the fuel injector, the volume is calculated to be

$$V = 5.34 \times 10^{-3} \text{ m}^3$$

The density of the kerosene is  $790 \text{ kg/m}^3$ . By using this, and assuming the mean temperature is  $1500 \text{ K}$ , we get a mean ab-

sorption coefficient of  $30 \text{ m}^{-1}$  [from Eqs. (A4) and (A5)] for  $C_s = 17 \text{ g/m}^3$  and the single-scattering albedo is 0.5. The number density and the mass of air and fuel are obtained as

$$N_D = 1.65 \times 10^{10} \text{ m}^{-3}, \quad m_a = 1.25 \times 10^{-2} \text{ kg},$$

$$m_f = 5.70 \times 10^{-4} \text{ kg}$$

Then, the fuel-air and equivalence ratios can be calculated as

$$\text{Fuel/air ratio} = m_f/m_a = \text{FA} = 4.60 \times 10^{-2}$$

$$\text{Equivalence ratio} = \phi = (\text{FA})/(\text{FA})_s = 0.67$$

For  $\omega = 0.9$ , the same analysis gives an equivalence ratio of 1.21 which is more reasonable. This indicates that if there are scattering kerosene droplets, then the probable range of single-scattering albedo would be from 0.5 to 0.9. Similar ranges would also be obtained for R25 and R50 fuels. Note that the stoichiometric fuel/air ratios  $(\text{FA})_s$  for kerosene, R25, and R50 fuels are  $6.87$ ,  $6.99$ , and  $7.04 \times 10^{-2}$ , respectively.<sup>4</sup>

### References

- <sup>1</sup>Lefebvre, A.H., "Flame Radiation in Gas Turbine Combustion Chambers," *International Journal of Heat and Mass Transfer*, Vol. 27, Sept. 1984, pp. 1493-1510.
- <sup>2</sup>Viskanta, R., "Radiative Heat Transfer," *Fortschritte der Verfahrenstechnik*, Vol. 22, Sec. A, 1984, pp. 51-81.
- <sup>3</sup>Mengüç, M.P. and Viskanta, R., "Radiative Transfer in Finite, Axisymmetric Cylindrical Enclosures," *Fundamentals of Thermal Radiation Heat Transfer*, edited by T.C. Min and J.L.S. Chen, ASME, New York, 1984, pp. 21-28.
- <sup>4</sup>Najjar, Y.S.H. and Goodger, E.M., "Radiation and Smoke from the Gas Turbine Combustor Using Heavy Fuels," *Journal of Heat Transfer*, Vol. 105, Feb. 1983, pp. 82-88.
- <sup>5</sup>Kuznar, R.J., Tobery, E.W., and Cohn, A., "Combustor Flame Radiation and Wall Temperatures for #2 Distillate and a Coal Derived Liquid Fuel," ASME Paper 82-GT-208, 1982.
- <sup>6</sup>Claus, R.W., Neely, G.M., and Humenik, F.M., "Flame Radiation and Liner Heat Transfer in a Tubular-Can Combustor," NASA TM 83538, 1984.
- <sup>7</sup>Ozisik, M.N., *Radiative Transfer and Interactions with Conduction and Convection*, John Wiley & Sons, New York, 1973.
- <sup>8</sup>Mengüç, M.P. and Viskanta, R., "Radiative Transfer in Three-Dimensional Rectangular Enclosures Containing Inhomogeneous, Anisotropically Scattering Media," *Journal of Quantitative Spectroscopy and Radiative Transfer*, Vol. 33, June 1985, pp. 533-549.
- <sup>9</sup>Rice, J.R. and Boisvert, R.F., *Solving Elliptic Problems Using ELLPACK*, Springer-Verlag, New York, 1984.
- <sup>10</sup>Najjar, Y.S.H., "Engineering Predictions of Soot Concentration in the Primary Zone of the Gas Turbine Combustor," *Journal of the Institute of Fuel*, Vol. 64, March 1985, pp. 93-98.
- <sup>11</sup>van de Hulst, H.C., *Light Scattering by Small Particles*, John Wiley & Sons, New York, 1957.
- <sup>12</sup>Sarofim, A.F. and Hottel, H.C., "Radiative Transfer in Combustion Chambers: Influence of Alternative Fuels," *Heat Transfer 1978*, Vol. 6, National Research Council of Canada, Ottawa, 1978, pp. 194-217.
- <sup>13</sup>Lefebvre, A.H. and Herbert, M.V., "Heat Transfer Processes in Gas-Turbine Combustion Chamber," *Proceedings of the Institute of Mechanical Engineers*, Vol. 174, Dec. 1960, pp. 463-473.
- <sup>14</sup>Lefebvre, A.H., *Gas Turbine Combustion*, McGraw-Hill Book Co., New York, 1983.